JOURNAL OF SOLID STATE CHEMISTRY 78, 281–293 (1989)

Spin-Glass Behavior in Sr_2FeRuO_6 and $BaLaNiRuO_6$: A Comparison with Antiferromagnetic $BaLaZnRuO_6$

P. D. BATTLE,* T. C. GIBB, AND C. W. JONES

Department of Inorganic and Structural Chemistry, The University, Leeds LS2 9JT, England

AND F. STUDER

Laboratoire CRISMAT, Associé au CNRS-UA251, Campus II, Boulevard du Maréchal Juin, ISMRa, Université de Caen, 14032 Caen Cedex, France

Received August 2, 1988

The crystal structures of the double perovskites $BaLaZnRuO_6$, $BaLaNiRuO_6$, and Sr_2FeRuO_6 have been refined in space group $I2/c$ using neutron powder diffraction data collected at room temperature. Data collected at 5 K led to refinements in $I2/c$ for Sr_2FeRuO_6 and $BaLaZnRuO_6$, and in a triclinic space group for $BaLaNiRuO_6$. $BaLaZnRuO_6$ shows A-type antiferromagnetism at 5 K whereas Sr_2FeRuO_6 and $BaLaNiRuO_6$ show no evidence of long-range magnetic ordering. Mössbauer and magnetic susceptibility data indicating low temperature transitions (<50 K) in these latter two materials have been interpreted in terms of spin-glass behavior, attributable to the long-range structural disorder of the B-site cations in the perovskite structure.

Introduction

Low-temperature antiferromagnetism has been observed in many compounds having the general formula $A_2BRu^{5+}O_6$ where A and B are diamagnetic cations (*1–4*). The materials studied to date all adopt a perovskite-related structure with an alternate ordering of the cations B and Ru^{5+} on the octahedral sites. The magnetic Ru^{5+} ions ($4d^3$:$^4A_{1g}$) thus form a face-centered array in a cubic unit cell having $a_0 \sim 8$ Å, that is $\sim 2a_p$ where a_p is the cell parameter of the primitive perovskite unit cell. These compounds frequently exhibit small distortions from cubic symmetry, but the octahedral sites always form a highly symmetrical array. A segment of a typical crystal structure with some distortion is shown in Fig. 1; the size of the unit cell is $\sim 5.5 \times 5.5 \times 8$ Å, that is $\sim\sqrt{2}a_p \times \sqrt{2}a_p \times 2a_p$. The arrangement of the magnetic ions in the corresponding 8-Å pseudo-cubic cell is shown in Fig. 2; the arrows in this diagram represent the alignment of the magnetic moments in the antiferromagnetic phase of all the compounds studied to date with the exception of Ba_2LaRuO_6. This spin arrangement, known as Type I antiferromagnetism, involves a strong antiferromagnetic superexchange interaction between nearest-neighbor (NN) Ru^{5+} ions and a negligible

* To whom correspondence should be addressed.

0022-4596/89 $3.00

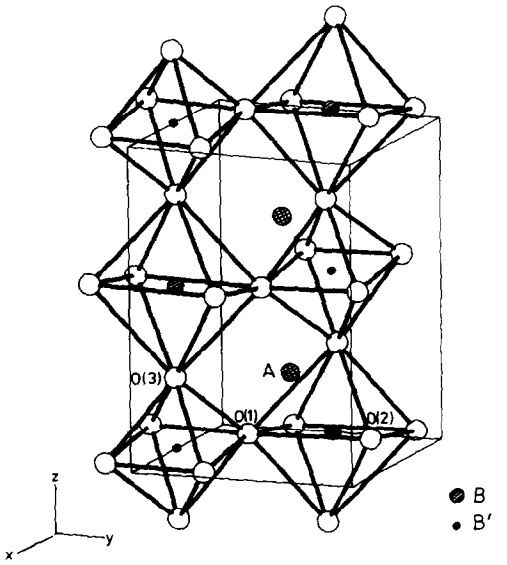

FIG. 1. The crystal structure of an ordered perovskite A_2BRuO_6. A and B are diamagnetic cations in 12- and 6-coordinate sites, respectively.

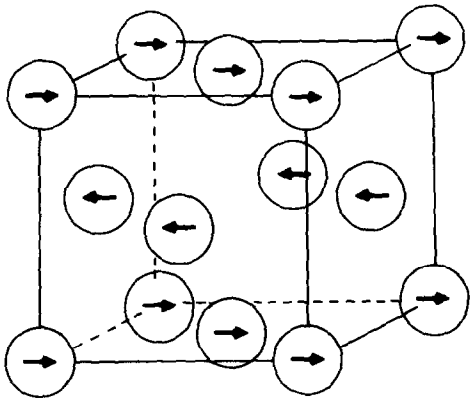

FIG. 2. Type I spin arrangement in antiferromagnetic A_2BRuO_6. Only the Ru^{5+} ions are marked; they occupy half the octahedral sites of the perovskite structure.

next-nearest-neighbor (NNN) interaction. The Type IIIa ordering adopted by Ba_2LaRuO_6 is consistent with a strong NN interaction over a distance of $\sim\sqrt{2}a_p$, but in this case there is also a significant antiferromagnetic NNN interaction over a distance of $\sim 2a_p$ (*1*).

In this paper we describe the consequences of introducing a second transition metal species into the structure, such that all the octahedral sites are occupied by magnetic ions. Conventional wisdom has it that under such circumstances the superexchange between NN cations, now separated by a distance of only a_p, will be by far the strongest magnetic interaction, and this is consistent with the observation of G-type antiferromagnetism (Fig. 3) below 750 K in $LaFeO_3$ (*5*). However, the compounds chosen for our study, $BaLaNiRuO_6$ and Sr_2FeRuO_6, present additional complications in that although 180° superexchange interactions between pairs of like ions (i.e., Ni/Ni, Fe/Fe, and Ru/Ru) are expected to be antiferromagnetic, those between a Ni/Ru pair are predicted to be ferromagnetic (*6*); in the case of an Fe/Ru pair, the 180° σ-superexchange is predicted to be ferromagnetic whereas the 180° π-superexchange is predicted to be antiferromagnetic. Furthermore, we are dealing with the interaction of electrons in 3*d* orbitals with those in 4*d* or-

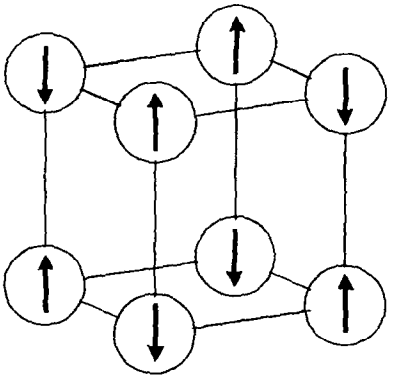

FIG. 3. G-type spin arrangement in an antiferromagnetic cubic perovskite with all the octahedral sites occupied by a magnetic cation. Only one octant of the unit cell is shown.

bitals, which have a more extensive wave function containing an extra radial node. In order to provide a reference point, we have also studied $BaLaZnRuO_6$, which contains a diamagnetic ion, Zn^{2+}, having a size comparable to that of Ni^{2+} and Fe^{3+}, and the Ru^{4+} compound La_2NiRuO_6. The structural details of the latter have been published elsewhere (*7*), whereas the crystal and magnetic structures of the former compound are reported for the first time below.

Sr_2FeRuO_6, $BaLaNiRuO_6$, and $BaLaZnRuO_6$ have all been prepared previously (*8, 9*). On the basis of X-ray powder patterns, Sr_2FeRuO_6 was reported to be a distorted perovskite-like phase with no ordering of the Fe^{3+} and Ru^{5+} ions on the octahedral sites. The cation oxidation states were established by Mössbauer spectroscopy; the ^{57}Fe spectrum was a quadrupole-split doublet at room temperature and a six-line pattern at 4.2 K ($\delta = 0.55$ mm sec^{-1}, $B = 49.1$ T), and the ^{99}Ru spectrum showed an 18-line hyperfine splitting at 4.2 K. The linewidths in the ^{57}Fe spectrum collected at 4.2 K were broad, consistent with a disordered cation arrangement. Magnetic susceptibility data collected in the range $80 < T < 300$ K indicated paramagnetism, although the Weiss constant θ was large and negative. These results were taken as evidence that Sr_2FeRuO_6 orders antiferromagnetically with $4.2 < T_N < 80$ K. The ^{99}Ru Mössbauer spectrum of $BaLaNiRuO_6$ also showed hyperfine splitting at 4.2 K and the magnetic susceptibility was found to reach a maximum at ~25 K, although the Weiss constant was positive. The low-temperature phase was again assumed to be antiferromagnetic, although it was recognized that a positive value of θ was anomalous in such a compound. X-ray powder diffraction patterns of $BaLaNiRuO_6$ and $BaLaZnRuO_6$ led Fernandez *et al.* (*9*) to conclude that both of these compounds are cubic, space group $Fm3m$, with an ordered 1 : 1 arrangement of cations on the octahedral sites. The ^{99}Ru Mössbauer spectrum of $BaLaZnRuO_6$ at 4.3 K was an 18-line hyperfine pattern, and the magnetic susceptibility had a maximum value at ~20 K. Significantly, and in contrast to $BaLaNiRuO_6$, the Weiss constant of $BaLaZnRuO_6$ was found to be large and negative. Again it was concluded that the susceptibility maximum corresponds to a transition between paramagnetic and antiferromagnetic phases.

In this paper we describe the determination of the full crystal structures of the title compounds by neutron powder diffraction, our attempts to establish their magnetic structures by low-temperature diffraction experiments, and the Mössbauer and susceptibility experiments that were prompted by our initial results. Finally, we interpret our data in terms of spin-glass behavior.

Experimental

Polycrystalline samples of the title compounds were prepared by firing the appropriate quantities of $BaCO_3$, La_2O_3, NiO, RuO_2, $SrCO_3$, and Fe_2O_3 (all spectroscopic-grade materials) in air at temperatures of 1300°C (Sr_2FeRuO_6) or 1350°C ($BaLaNiRuO_6$ and $BaLaZnRuO_6$) for several days, slow cooling to less than 800°C, and then quenching to room temperature. The mixtures were ground and remade into pellets several times during the course of the reactions, the progress of which was monitored by X-ray powder diffraction. This technique indicated that the final, well-sintered products were monophasic perovskites with symmetries lower than cubic. Neutron diffraction data were collected at room temperature and 5 K for all three compounds using the powder diffractometers D1a (Sr_2FeRuO_6 and $BaLaNiRuO_6$; $\lambda = 1.958$ or 1.910 Å) and D2b ($BaLaZnRuO_6$, $\lambda = 1.594$ Å) at ILL Grenoble operating with a 2θ step size of 0.05°. The samples were contained

in 12- or 16-mm-diameter vanadium cans. The resulting data were all analyzed by the profile analysis technique (*10*) using the following scattering lengths: $b_{Ba} = 0.52$, $b_{La} = 0.83$, $b_{Sr} = 0.69$, $b_{Ru} = 0.73$, $b_{Zn} = 0.57$, $b_{Fe} = 0.95$, $b_{Ni} = 1.03$, and $b_O = 0.58 \times 10^{-12}$ cm. The background levels were estimated by interpolation between regions where there were no Bragg peaks. ^{57}Fe Mössbauer spectra of Sr_2FeRuO_6 were recorded between room temperature and 4.2 K with a ^{57}Co/Rh source matrix at room temperature; isomer shift values are relative to the spectrum of metallic iron. Temperatures below 80 K were obtained using liquid helium in an Oxford Instruments CF500 continuous flow cryostat controlled by a DTC2 digital temperature controller. The main spectrometer was an MS102 microprocessor from Cryophysics Ltd. The magnetic susceptibilities of Sr_2FeRuO_6 and BaLaNi RuO_6 were recorded under both zero-field-cooled (zfc) and field-cooled (fc) conditions using an Aztec DSM5 Faraday magnetometer which had been calibrated using 99.999% pure Gd_2O_3. Approximately 120 mg of sample were held in a plastic container at the end of a quartz-tailed rigid brass rod, which was suspended between the poles of an electromagnet such that the sample experienced a mutually perpendicular magnetic field and field gradient, both in the plane perpendicular to the rod. An SMC-TBT helium flow cryostat controlled by a BT-300 temperature regulator was used to vary the temperature between 5 and 300 K with a stability of 0.2 K. All measurements were made in a field of 0.3 T, which was also the field applied during cooling in the case of the fc experiments.

Results

(*i*) *BaLaZnRuO*$_6$

The room-temperature neutron diffraction data from $BaLaZnRuO_6$ were analyzed in space group *I*2/*c*, that is, with a monoclinic distortion of the perovskite structure and with a disordered arrangement of Ru^{5+} and Zn^{2+} ions on the octahedral *B* sites, in contrast to the ordered cation arrangement shown in Fig. 1. Ba^{2+} and La^{3+} ions were assumed to be disordered over the *A* sites. Refinements of the usual profile parameters and the atomic parameters led to the agreement factors $R_{wpr} = 10.4\%$ and $R_I = 5.2\%$ when the highly asymmetric peaks with $2\theta < 40°$ were excluded from the analysis. The refined values of the atomic parameters and the most important bond lengths and bond angles are listed in Tables I and II, respectively. The final observed, calculated, and difference diffraction profiles are plotted in

TABLE I

STRUCTURAL PARAMETERS FOR $BaLaZnRuO_6$ AT ROOM TEMPERATURE (SPACE GROUP *I*2/*c*)

Atom	Site	*x*	*y*	*z*	*B* (Å^2)
Ba/La	4e	0	0.499(1)	1/4	0.57(3)
Zn/Ru	4a	0	0	0	0.23(3)
O1	4e	0	0.043(1)	1/4	1.49(4)
O2	8f	0.260(1)	0.752(2)	0.0190(6)	1.49(4)

Note. Cell parameters: $a = 5.6479(2)$, $b = 5.6672(2)$, $c = 7.9859(2)$ Å; $\beta = 90.10(1)°$.

TABLE II

BOND LENGTHS (IN Å) AND BOND ANGLES (IN DEGREES) FOR $BaLaZnRuO_6$ AT ROOM TEMPERATURE

Zn/Ru–O1	Zn/Ru–O2
2.011(6)	2.01(1)
	2.00(1)
Ba/La–O1	Ba/La–O2
2.587(8)	2.78(1)
3.081(8)	2.98(1)
2.834(8)	2.88(1)
	2.67(1)
O1–Zn/Ru–O2	90.5
O1–Zn/Ru–O2	90.7
O2–Zn/Ru–O2	90.5

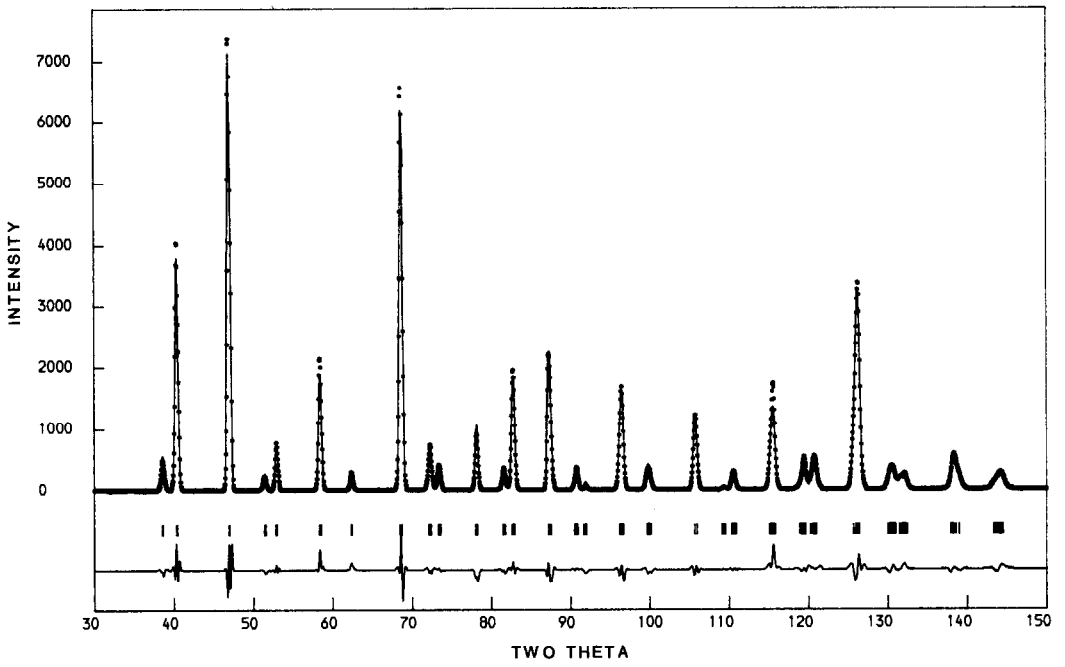

FIG. 4. The observed (. . .), calculated (—), and difference diffraction profiles of $BaLaZnRuO_6$ at room temperature. Reflection positions are marked.

Fig. 4. The unit cell parameters refined to the following values: a = 5.6479(2), b = 5.6672(2), c = 7.9859(2) Å, β = 90.10(1)°. Here, and throughout this paper, the figure in brackets is the estimated standard deviation in the last place. The data collected at 5 K contain additional Bragg peaks indicative of long-range Type A antiferromagnetic ordering (Fig. 5). The nonmagnetic scattering was analyzed in space group $I2/c$ and the final structural parameters are given in Table III (R_{wpr} = 10.2%, R_I = 4.8%). The magnitude of the ordered magnetic moment of the Ru^{5+} cations was then estimated by

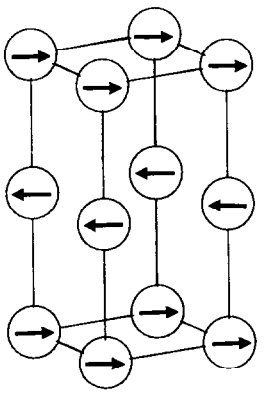

FIG. 5. A-type spin arrangement in an antiferromagnetic cubic perovskite with all the octahedral sites occupied by a magnetic cation.

TABLE III

STRUCTURAL PARAMETERS FOR $BaLaZnRuO_6$ AT 5 K (SPACE GROUP $I2/c$)

Atom	Site	x	y	z	B (Å^2)
Ba/La	4e	0	0.501(1)	1/4	0.65(2)
Zn/Ru	4a	0	0	0	0.39(2)
O1	4c	0	0.0432(9)	1/4	1.63(9)
O2	8f	0.261(1)	0.759(2)	0.0222(4)	1.58(5)

Note. Cell parameters: a = 5.6364(2), b = 5.6621(2), c = 7.9686(2) Å; β = 90.077(7)°.

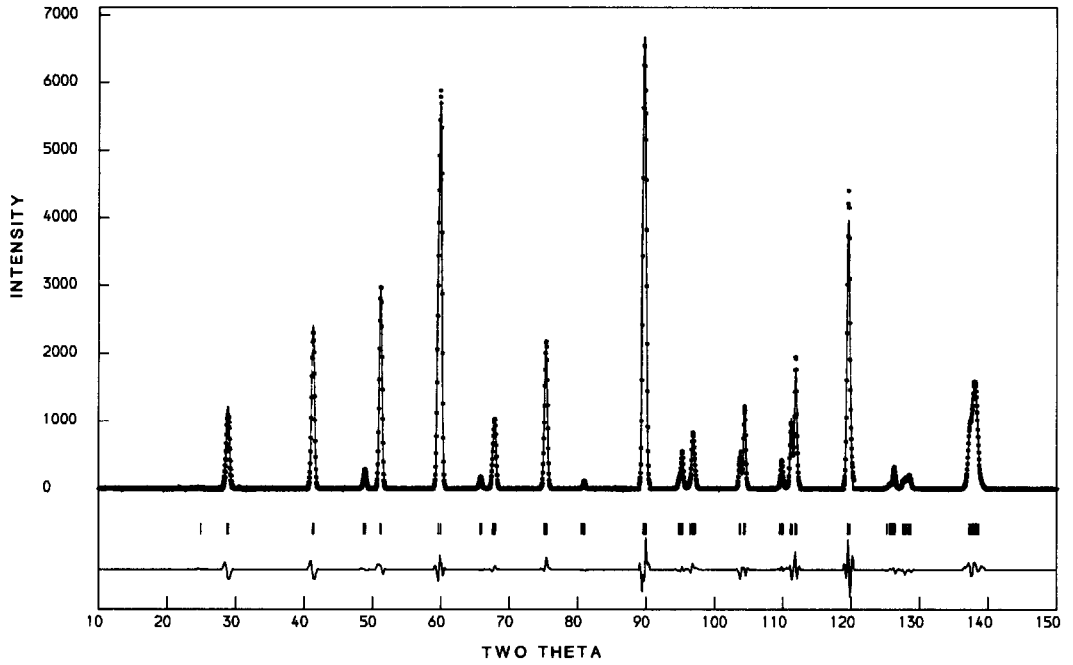

FIG. 6. The observed (. . .), calculated (—), and difference diffraction profiles of Sr_2FeRuO_6 at room temperature. Reflection positions are marked.

comparing the intensity of the strongest magnetic peak, (001), with that of several intense nonmagnetic peaks, assuming a value of unity for the form factor of Ru^{5+} at $\sin\theta/\lambda \sim 0.06$. We do not feel justified in including the very weak magnetic peaks at higher angles in a refinement because of uncertainties in the form factor. The magnetic moment calculated in this way was 1.5(1) μ_B per Ru^{5+}, in reasonable agreement with the values found previously in magnetically ordered oxides (*1–4*).

TABLE IV

STRUCTURAL PARAMETERS FOR Sr_2FeRuO_6 AT ROOM TEMPERATURE (SPACE GROUP *I2/c*)

Atom	Site	*x*	*y*	*z*	*B* (Å²)
Sr	4e	0	0.500(3)	1/4	0.53(4)
Fe/Ru	4a	0	0	0	0.48(4)
O1	4e	0	0.011(5)	1/4	0.98(9)
O2	8f	0.228(2)	0.728(2)	0.0055(8)	0.83(6)

Note. Cell parameters: $a = 5.5379(3)$, $b = 5.5429(3)$, $c = 7.8772(1)$ Å; $\beta = 90.11(1)°$.

(ii) Sr_2FeRuO_6

The full diffraction data set collected on Sr_2FeRuO_6 at room temperature was analyzed in space group *I2/c*. The diffraction profiles drawn in Fig. 6 derive from the structural parameters of Table IV and correspond to agreement factors $R_{wpr} = 9.4\%$ and $R_I = 3.8\%$. The corresponding bond lengths and bond angles are listed in Table V. The data collected at 5 K were analyzed in a similar way, leading to the structural parameters presented in Table VI with $R_{wpr} = 10.8\%$ and $R_I = 5.2\%$. There were no peaks in the low-temperature data set that could be attributed to magnetic scattering, nor was there a marked enhancement of any of the peaks which are common to both data sets. The 5 K data were thus analyzed in terms of nuclear scattering alone.

TABLE V

BOND LENGTHS (IN Å) AND BOND ANGLES (IN DEGREES) FOR Sr_2FeRuO_6 AT ROOM TEMPERATURE

Fe/Ru–O1		Fe/Ru–O2	
1.97(3)		1.97(2)	
		1.97(2)	
Sr–O1		Sr–O2	
2.72(3)		2.63(2)	
2.83(3)		2.69(2)	
2.78(3)		2.93(2)	
		2.87(2)	
O1–Fe/Ru–O2	90.1	Fe/Ru–O1–Fe/Ru	176.6
O1–Fe/Ru–O2	90.3	Fe/Ru–O2–Fe/Ru	169.7
O2–Fe/Ru–O2	90.1		

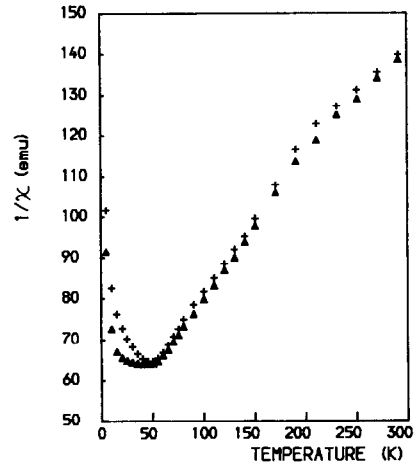

FIG. 7. The inverse molar magnetic susceptibility of Sr_2FeRuO_6 as a function of temperature (+, zfc; Δ, fc).

The inverse molar magnetic susceptibility of Sr_2FeRuO_6 is shown in Fig. 7, for both the zfc and fc cases. The zfc curve has a minimum at ~50 K. Above this temperature $1/\chi$ increases in a nonlinear manner, the gradient of the graph decreasing with increasing temperature. In the temperature range $80 < T < 200$ K, the molar Curie constant is approximately 2.8; for $200 < T < 300$ K the value has increased to ~4.3. The effective magnetic moment per cation thus increases from ~3.4 to ~4.2 μ_B, but is always below the average value (5 μ_B) expected for a random, noninteracting arrangement of Ru^{5+} and Fe^{3+} ions. It is clear from Fig. 7 that the Weiss constant, θ, for Sr_2FeRuO_6 is large and negative, indicative of the presence of antiferromagnetic interactions. The fc susceptibility overlays the zfc curve above 50 K. However, below this temperature $\chi_{fc} > \chi_{zfc}$.

TABLE VI

STRUCTURAL PARAMETERS FOR Sr_2FeRuO_6 AT 5 K (SPACE GROUP *I2/c*)

Atom	Site	*x*	*y*	*z*	*B* (Å^2)
Sr	4e	0	0.501(2)	1/4	0.62(4)
Fe/Ru	4a	0	0	0	0.68(4)
O1	4e	0	0.006(4)	1/4	0.94(7)
O2	8f	0.219(1)	0.724(1)	0.0074(6)	0.84(5)

Note. Cell parameters: $a = 5.5092(3)$, $b = 5.5138(3)$, $c = 7.8752(1)$ Å; $\beta = 90.13(1)°$.

The Mössbauer spectrum of Sr_2FeRuO_6 is plotted as a function of temperature in Fig. 8. At 290 K the spectrum consists of a simple quadrupole doublet with a chemical shift of $\delta = 0.37$ mm sec^{-1}, and a quadrupole splitting of $\Delta = 0.60$ mm sec^{-1}. The linewidth of $\Gamma = 0.53$ mm sec^{-1} is larger than normal because of the variable effect of the incipient cation disorder on the electric field gradient at any given iron site. Below approximately 70 K this simple spectrum broadens out and is eventually replaced by a six-line magnetic hyperfine splitting. At 4.2 K, the hyperfine field has a flux density of 49.0 T and an isomer shift of 0.51 mm sec^{-1}. The pattern is symmetrical as if there were no quadrupole interaction, but the linewidth is large at 0.73 mm sec^{-1} and it may be assumed that the electric field gradient tensor can take up a number of different orientations with respect to the spin axis. The Mössbauer parameters are typical of Fe^{3+} cations. As the temperature increases the magnetic flux density begins to decrease in the characteristic Brillouin

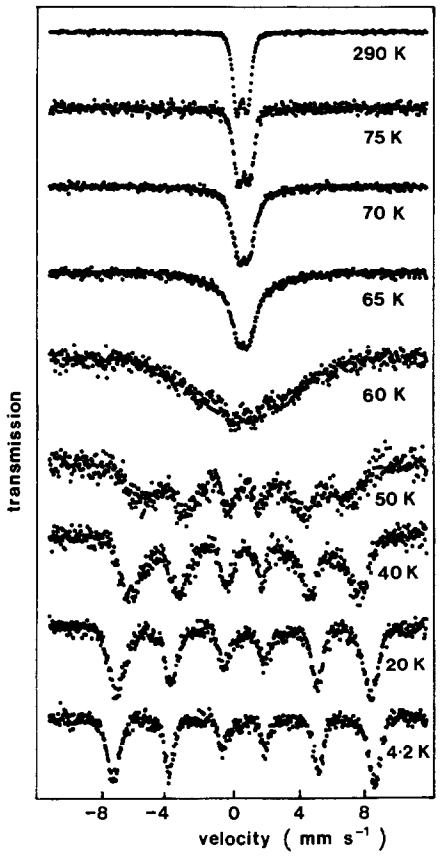

FIG. 8. The Mössbauer spectrum of Sr_2FeRuO_6 as a function of temperature between 290 and 4.2 K.

collapse of a magnetically ordered material, but by 40 K there is a very marked increase in the linewidth. As the temperature increases further there is an inward collapse of the hyperfine pattern suggestive of a relaxational motion of the spin axis. There is no distinct ordering temperature as would be found in a simple antiferromagnet, for example, nor is the relaxation behavior compatible with slow paramagnetic relaxation which does not show an initial Brillouin collapse.

(iii) $BaLaNiRuO_6$

As in the cases of $BaLaZnRuO_6$ and Sr_2FeRuO_6, the room-temperature crystal structure of this compound was refined in space group *I*2/*c* with a disordered arrangement of Ru and the first-row transition metal on the octahedral sites. The refined structural parameters are listed in Table VII and bond lengths and bond angles are given in Table VIII. The observed, calculated, and difference profiles are plotted in Fig. 9, for agreement factors of R_{wpr} = 9.3%, R_I = 4.6%. However, we were unable to obtain satisfactory refinements of the crystal structure at 5 K in a monoclinic space group and we therefore lowered the symmetry to triclinic, while retaining an *I*-centered cell for ease of comparison with the other structures discussed in this paper.

TABLE VII

STRUCTURAL PARAMETERS FOR $BaLaNiRuO_6$ AT ROOM TEMPERATURE (SPACE GROUP *I*2/*c*)

Atom	Site	*x*	*y*	*z*	*B* (Å^2)
Ba/La	4e	0	0.498(3)	1/4	0.45(4)
Ni/Ru	4a	0	0	0	0.33(4)
O1	4e	0	−0.013(4)	1/4	1.5(2)
O2	8f	0.222(2)	0.726(2)	0.0090(7)	1.02(8)

Note. Cell parameters: a = 5.6093(3), b = 5.6154(3), c = 7.9571(2) Å; β = 90.16(1)°.

TABLE VIII

BOND LENGTHS (IN Å) AND BOND ANGLES (IN DEGREES) FOR $BaLaNiRuO_6$ AT ROOM TEMPERATURE

Ni/Ru–O1	Ni/Ru–O2
1.99(2)	1.98(2)
	2.01(2)
Ba/La–O1	Ba/La–O2
2.87(3)	2.63(2)
2.75(3)	2.72(2)
2.81(3)	3.00(2)
	2.91(2)
O1–Ni/Ru–O2	93.6
O1–Ni/Ru–O2	93.5
O2–Ni/Ru–O2	90.2

TABLE IX

STRUCTURAL PARAMETERS FOR $BaLaNiRuO_6$ AT 5 K (SPACE GROUP $I\bar{1}$)

Atom	x	y	z	B (Å^2)
Ba/La	0.000(4)	0.501(1)	0.246(4)	0.43(6)
Ni/Ru(1)	0	0	0	0.49(4)
Ni/Ru(2)	0	0	1/2	0.49(4)
O1	0.016(6)	−0.015(7)	0.248(5)	1.07(5)
O2	0.229(7)	0.726(6)	0.004(6)	1.07(5)
O3	−0.213(6)	0.716(5)	0.492(2)	1.07(5)

Note. Cell parameters: a = 5.5964(2), b = 5.5879(2), c = 7.9319(1) Å; α = 89.803(7), β = 90.10(2), γ = 90.09(1)°.

TABLE X

BOND LENGTHS (IN Å) AND BOND ANGLES (IN DEGREES) FOR $BaLaNiRuO_6$ AT 5 K

Ni/Ru(1)–O1	1.97(7)	Ni/Ru(2)–O1	2.00(7)
Ni/Ru(1)–O2	2.00(7)	Ni/Ru(2)–O2	1.98(7)
Ni/Ru(1)–O3	2.01(5)	Ni/Ru(2)–O3	1.98(5)
Ba/La–O1	Ba/La–O2	Ba/La–O3	
2.89(8)	2.63(8)	2.59(6)	
2.71(8)	2.69(8)	2.68(6)	
2.89(8)	2.97(8)	3.04(6)	
2.71(8)	2.92(8)	2.94(6)	
O1–Ni/Ru(1)–O2	94.3	O1–Ni/Ru(2)–O2	94.7
O1–Ni/Ru(1)–O3	91.3	O1–Ni/Ru(2)–O3	92.4
O1–Ni/Ru(1)–O3	93.0	O2–Ni/Ru(2)–O3	93.0

The final structural parameters are given in Table IX; they correspond to the agreement factors R_{wpr} = 9.6%, R_I = 4.2%. The bond distances in the triclinic structure are listed in Table X. The inverse molar magnetic susceptibility of $BaLaNiRuO_6$ is plotted in Fig. 10. These curves differ in a number of ways from those presented for Sr_2FeRuO_6 in Fig. 7. There is little difference between the zfc and fc susceptibilities, both having a maximum at ~20 K. The gradient of $1/\chi$ versus T increases as the temperature is increased toward 300 K and hence the effective magnetic moment per cation de-

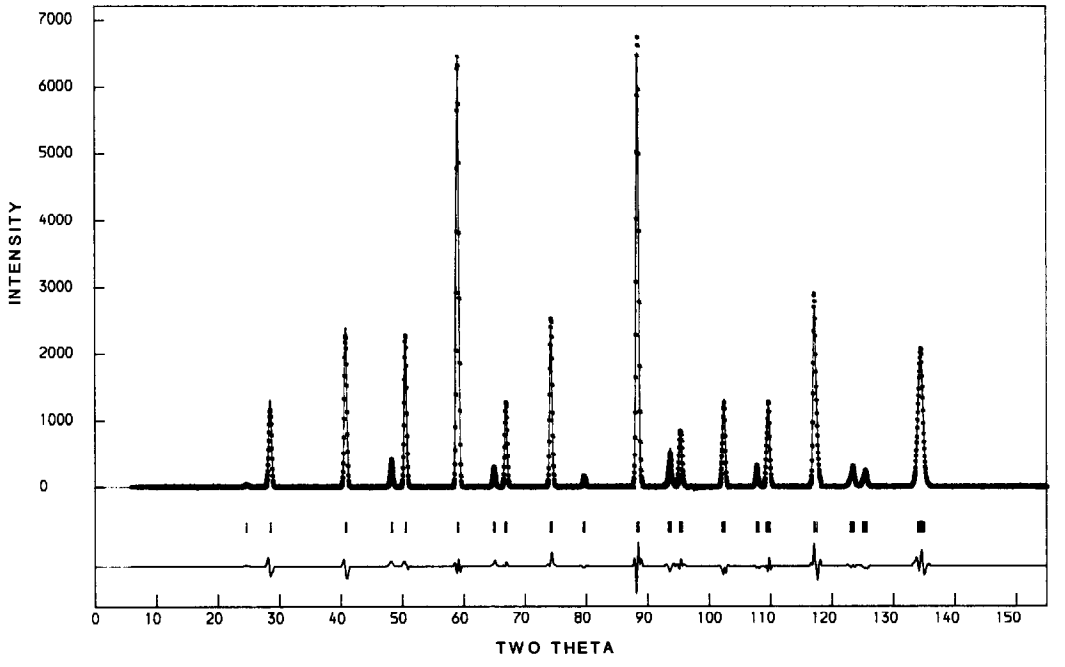

FIG. 9. The observed (. . .), calculated (—), and difference diffraction profiles of $BaLaNiRuO_6$ at room temperature. Reflection positions are marked.

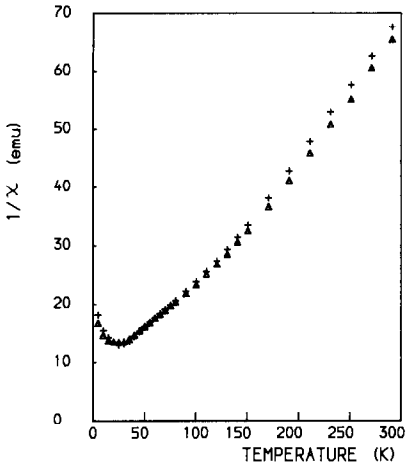

FIG. 10. The inverse molar magnetic susceptibility of $BaLaNiRuO_6$ as a function of temperature (+, zfc, Δ, fc).

creases, in contrast to the behavior of Sr_2FeRuO_6. The Curie constant for $150 < T < 300$ K is ~4.1 and hence the average effective moment per cation is ~4 μ_B, larger than the value of ~3.4 μ_B expected on the basis of the spin-only formula. The Weiss constant, θ, deduced from the high temperature data is small (~20 K) and positive, in agreement with the results of Fernandez *et al.* (*9*).

Discussion

The crystal structures described above are all strongly pseudo-symmetric, particularly Sr_2FeRuO_6, and the space group *I*2/*c* was only accepted after refinements in space groups of higher symmetry had produced poor agreement between the observed and calculated diffraction profiles. The pseudo-symmetry manifests itself in relatively high standard deviations associated with the metal–oxygen bond distances listed in the tables; a similar effect was found in Ba_2LaRuO_6 (*1*), a pseudo-cubic triclinic compound. The presence of the subtle distortions necessitated the omission of the grossly asymmetric, low-angle peaks from the analysis of the data collected on D2b for $BaLaZnRuO_6$, although we were able to work with the full data sets collected on D1a for Sr_2FeRuO_6 and $BaLaNiRuO_6$. An important feature of all three compounds is the lack of long-range order among the transition metal species which occupy the 6-coordinate sites. This is in accord with our previous work on La_2NiRuO_6 (*7*), but contradicts the conclusions drawn by Fernandez *et al.* (*9*) from a qualitative inspection of X-ray powder diffraction patterns. Support for a disordered arrangement comes from the low-temperature structure of $BaLaNiRuO_6$, which was refined in space group $I\bar{1}$, thus making cation ordering possible. However, the oxide ions refined to positions which create two octahedral sites of essentially the same size, consistent with a disordered cation distribution. The *M*/Ru–O bond lengths in all three of the title compounds (*M* = Fe, Ni, or Zn) are intermediate between those expected for Ru^{5+}–O and *M*–O bonds, again consistent with a lack of long-range order. The bonds in $BaLaNiRuO_6$ are somewhat shorter than those found in La_2NiRuO_6, consistent with the Ru ions in the latter having an oxidation state of +4 rather than +5 as in the former. The oxygen–oxygen distances (not tabulated) in all three compounds are typical of mixed-metal oxides, the shortest contact at room temperature being 2.72 Å.

The magnetic behavior of these materials is most unusual and merits careful attention. The perovskite $Sr_2Fe^{3+}Mo^{5+}O_6$ (*11*) is ferrimagnetically ordered below 450 K. However, the *B*-site cations in this compound are ordered, unlike those in our samples, and we shall show below how the magnetic properties of these materials are controlled by cation ordering. It is interesting to note that the temperature factors of atoms O1 and O2 in $BaLaZnRuO_6$ are unusually high, and the enhanced values per-

sist down to 5 K. This indicates either that there is a significant vacancy concentration in the oxygen sublattice or that the oxide ions undergo small displacements from their ideal positions. Our attempts to refine the occupation factors of O1 and O2 failed to improve the agreement between the observed and calculated profiles. The idea of small anion displacements is attractive when considered along with the magnetic properties of $BaLaZnRuO_6$. The Zn^{2+} and Ru^{5+} cations are apparently disordered over the octahedral sites of a perovskite structure; in effect they form a pseudo-cubic primitive arrangement with half of the sites occupied by a magnetic cation. With such a high concentration of magnetic species, well above the percolation limit, it is entirely reasonable for the compound to order antiferromagnetically at low temperatures; what is surprising is the nature of the magnetic structure that is adopted. We would expect the NN superexchange along a pathway Ru–O–Ru to be the strongest magnetic interaction in such a system, and that a *G*-type magnetic structure would be adopted, as in the case of $LaFeO_3$ (*5*) cited above. However, the adoption of an *A*-type structure indicates that the Ru–Ru interaction over a distance $\sqrt{2}a_p$ is dominant, that is, the same interaction that dominates in the A_2BRuO_6 compounds having an ordered arrangement of *B* and Ru^{5+} ions. We therefore propose that, although the Zn^{2+} and Ru^{5+} ions are disordered over the distances sampled in a neutron diffraction experiment, *short-range order* increases the number of Ru–O–Zn NN pathways and the number of NNN Ru–Ru interactions to such an extent that Type *A* ordering is more stable than Type *G*. This local cation ordering will produce corresponding anion displacements, consistent with the enhanced temperature factors discussed above. There is thus no major unexplained conflict between the neutron diffraction, Mössbauer, and susceptibility data on Ba $LaZnRuO_6$; the compound orders antiferromagnetically at low temperatures in a way which is consistent with the crystal structure if we invoke the presence of short-range ordering of the *B*-site cations. It is interesting to note that Sr_2FeNbO_6, another compound with a disordered arrangement of cations in the octahedral sites, does not order antiferromagnetically but behaves as a spin glass (*12*). It has been suggested that short-range ordering is present in this compound, and that it raises the effective percolation threshold for *G*-type magnetic ordering. Apparently the adoption of a Type *A* structure is not open to Sr_2FeNbO_6, possibly because of the relatively small radial extent of the 3*d* orbitals on Fe^{3+} compared to that of the 4*d* orbitals on Ru^{5+}.

The case of Sr_2FeRuO_6 is more complex than that of $BaLaZnRuO_6$. The Mössbauer and the zfc susceptibility data suggest that this compound may be antiferromagnetic at 5 K. However, the behavior of the fc susceptibility, the non-Brillouin collapse of the ^{57}Fe Mössbauer spectrum at 50 K, and the absence of magnetic scattering from the low-temperature diffraction pattern all indicate that this is an incorrect conclusion. The hyperfine splitting in both the ^{99}Ru and ^{57}Fe Mössbauer spectra at 4.2 K indicates that the cation spins are static on a timescale of $\sim 10^{-7}$ sec, but the absence of magnetic Bragg peaks proves that there is no long-range magnetic ordering. We therefore conclude that we are dealing with a spin glass, and this conclusion is supported by the magnetic susceptibility data. The reduced effective magnetic moment at high temperatures reflects the occurrence of short-range antiferromagnetic clustering; as the temperature is lowered the number and size of the clusters increases until at the glass transition temperature, $T_G \sim 45$ K, an infinite cluster is formed and, on further cooling, the fc and zfc susceptibilities diverge. This model is consistent with that proposed previously for Sr_2FeNbO_6 (*12*),

and also with the theoretical work of Barbara and Malozemoff (*13*) and Cyrot (*14*). It is, however, unusual for an insulating material having a nonfrustrated primitive pseudo-cubic lattice, fully occupied by magnetic cations, to behave in such a way. Our explanation of the behavior relies on the existence of a ferromagnetic superexchange interaction between $4d^3$:Ru^{5+} and $3d^5$:Fe^{3+} ions. Indeed the occurrence of antiferromagnetic ordering in $BaLaZnRuO_6$ and spin-glass behavior in Sr_2FeRuO_6 indicates that the interactions between the second magnetic species and the Ru^{5+} ions are crucial for the formation of a glassy phase. The magnetic interaction between pairs of Fe^{3+} ions will always be antiferromagnetic in this structure, as will that between pairs of Ru^{5+} ions. Given the high Néel temperature of $LaFeO_3$, it is easy to visualize short-range antiferromagnetic spin-ordering between neighboring Fe^{3+} ions in Sr_2FeRuO_6 at room temperature, and hence to explain the reduced magnetic moment at high temperatures. At lower temperatures, the extent of this short-range order will increase, and a similar effect will begin to occur between neighboring Ru^{5+} ions. However, there will also be a ferromagnetic σ-interaction along all connections of the form Ru–O–Fe. This interaction is strongest when the superexchange pathway is linear, and in Sr_2FeRuO_6 the departure from linearity is small (Ru–O–Fe $\geq$ 170°). The growth of antiferromagnetic clusters will be opposed by this interaction, and below T_G an infinite cluster is formed with all spins static in a topologically nonfrustrated arrangement which contains antiferromagnetic pairs of like ions and ferromagnetic Ru/Fe pairs. However, because the Ru^{5+} and Fe^{3+} ions are arranged randomly over the lattice sites, there will be no long-range order of the spins and consequently only weak, unobservable magnetic peaks in the neutron powder diffraction pattern. There are many examples of spin-glass behavior in insulating materials having a topologically frustrated lattice (*15*) or competing NN and NNN interactions (*16*) but, to our knowledge, Sr_2FeRuO_6 and $BaLaNiRuO_6$ (to be discussed below) are the first compounds having a nondiluted, nonfrustrated magnetic sublattice which shows spin-glass behavior.

There are both similarities and differences between the magnetic behavior of Sr_2FeRuO_6 and that of $BaLaNiRuO_6$. In the latter case, Fernandez *et al.* (*9*) have observed hyperfine splitting in the ^{99}Ru Mössbauer spectrum at 4.2 K, but we do not see any magnetic scattering in the neutron diffraction pattern. These results suggest that $BaLaNiRuO_6$ is also a spin glass, but the magnetic susceptibility results necessitate a more careful analysis. There is no significant difference between the zfc and fc data at temperatures below the susceptibility maximum, but this may be a consequence of the field used (0.3 T). A more important difference between the data collected on $BaLaNiRuO_6$ and those from Sr_2FeRuO_6 is that whereas the effective magnetic moment of the latter is always less than the spin-only value, that of the former is enhanced between T_G and 300 K. This implies that any short-range ordering is ferromagnetic, consistent with a positive value of θ, but the presence of a minimum in $1/\chi$ versus T suggests that an antiferromagnetic ordering takes place at ~20 K. Similar behavior has been observed in $Fe_xMg_{1-x}Cl_2$ (*17*) by Bertrand *et al.* who proposed that ferromagnetic clusters develop at high temperatures and that these clusters interact antiferromagnetically at T_G. Their data, like ours, extrapolate to a positive θ value from high temperatures and to a negative value from the temperature range immediately above T_G. We must therefore explain why the short-range ordering which occurs at high temperatures in $BaLaNiRuO_6$ is predominantly ferromagnetic. As in the case of Sr_2FeRuO_6, the superexchange between pairs of like ions (Ni/Ni or Ru/Ru) will be antiferromagnetic. However, 180° superex-

change along a pathway Ni^{2+}–O–Ru^{5+} is predicted (*6*) to be ferromagnetic for both σ- and π-orbitals, and it appears that this interaction dominates the high-temperature short-range ordering in our compound where the bond angle is $\geq 168°$. This is surprising because Ni–O–Ni antiferromagnetic superexchange is known to be very strong, leading to a Néel temperature of 523 K in NiO (*18*). In order to rationalize our observations, we suggest that in $BaLaNiRuO_6$, as in $BaLaZnRuO_6$, there is a local 1 : 1 ordering of the 6-coordinate cations, and the number of Ni–O–Ru pathways is thus increased above that expected in a truly disordered structure. This hypothesis is once again supported by the large temperature factors of the oxide ions (see Table VII), a feature which was absent in Sr_2FeRuO_6 where we did not invoke short-range order to explain the magnetic properties. It is entirely reasonable that ordering should occur to a small extent between Ru^{5+} and Ni^{2+} or Zn^{2+}, but not between Ru^{5+} and the smaller, more highly charged Fe^{3+} ions.

In conclusion, we have presented experimental evidence which suggests that $BaLaNiRuO_6$ and Sr_2FeRuO_6 show spin-glass behavior at low temperatures. These materials need to be investigated further using ac susceptibility techniques and diffuse elastic neutron scattering, the latter to probe short-range ordering, both structural and magnetic.

Acknowledgments

We acknowledge the SERC for financial support and for a studentship (to C.W.J.). This collaboration arose following the appointment of P.D.B. as a Visiting Professor at ISMRa, Caen.

References

1. P. D. Battle, J. B. Goodenough, and R. Price, *J. Solid State Chem.* **46,** 234 (1983).
2. P. D. Battle and W. J. Macklin, *J. Solid State Chem.* **52,** 138 (1984).
3. P. D. Battle and W. J. Macklin, *J. Solid State Chem.* **54,** 245 (1984).
4. P. D. Battle and C. W. Jones, *J. Solid State Chem.* **78,** 108 (1989).
5. W. C. Koehler and E. O. Wollan, *J. Phys. Chem. Solids* **2,** 100 (1957).
6. J. B. Goodenough, "Magnetism and the Chemical Bond," Wiley, New York (1963).
7. P. D. Battle and C. W. Jones, *Mater. Res. Bull.* **22,** 1623 (1987).
8. T. C. Gibb, R. Greatrex, N. N. Greenwood, and K. G. Snowden, *J. Solid State Chem.* **14,** 193 (1975).
9. I. Fernandez, R. Greatrex, and N. N. Greenwood, *J. Solid State Chem.* **32,** 97 (1980).
10. H. M. Rietveld, *J. Appl. Crystallogr.* **2,** 65 (1969).
11. S. Nakayama, T. Nakagawa, and S. Nomura, *J. Phys. Soc. Japan* **24,** 219 (1968).
12. R. Rodriguez, A. Fernandez, A. Isalgué, J. Rodriguez, A. Labarta, J. Tejada, and X. Obradors, *J. Phys. C: Solid State Phys.* **18,** L401 (1985).
13. B. Barbara and A. P. Malozemoff, *J. Less-Common Met.* **94,** 45 (1983).
14. M. Cyrot, *Solid State Commun.* **39,** 1009 (1981).
15. D. Fiorani, S. Viticoli, J. L. Dormann, J. L. Tholence, and A. P. Murani, *Phys. Rev. B* **30,** 2776 (1984).
16. M. Alba, J. Hammann, and M. Nogues, *J. Phys. C: Solid State Phys.* **15,** 5441 (1982).
17. D. Bertrand, F. Bensamka, A. R. Fert, J. Gelard, J. P. Redoules, and S. Legrand, *J. Phys. C: Solid State Phys.* **17,** 1725 (1984).
18. M. Foex, *C. R. Acad. Sci.* **227,** 193 (1948).